Turbulent Micromixing Parameters from Reactive Mixing Measurements

Previously published conversion data for turbulent diffusion-controlled acid-base reactions in two different multijet reactors are used to extract the mixing parameters, tracer probability density function, and variance. The PDF is obtained with this instantaneous reaction method by differentiating twice the reactive mixing plot of mean reactant concentrations. The limiting behavior for the cases of complete segregation and complete mixing is derived and turns out to be piecewise linear on the reactive mixing plot. The variance is shown to be twice the area between the actual reactive mixing curve and the limiting curve for complete mixing; it can be computed by numerical integration without any foreknowledge of the PDF shape. The method, in principle, allows detection of Dirac delta functions (which represent unmixed virgin fluid) and indeed shows significant amounts of virgin fluid close to the inlet of one of the reactors.

U.V. Shenoy
H.L. Toor
Department of Chemical Engineering
Carnegie Mellon University
Pittsburgh, PA 15213

The concentration uniformity or state of mixedness in a turbulent system can be quantified by a probability density function (PDF) which describes the fraction of the time or volume in which the nonreacting tracer concentration takes on a particular value. The mean, which is the first moment of the PDF, describes the state of macromixing, and the variance, which is the second moment, is a useful measure of the micromixing.

The PDF can be obtained by measuring the *instantaneous* values of an inert (passive) tracer—temperature or concentration (Brodkey, 1975). Since the finite probe volume sets a limit on resolution of the smallest length scales, this method overestimates the amount of mixing which takes place (Koochesfahani and Dimotakis, 1986).

Instantaneous chemical reaction can also be used to obtain the PDF with the advantage that only *mean* quantities need to be measured. The chemical indicator method, first proposed by Danckwerts (1957), mixes acid and base with a present chemical indicator and uses measurements of the mean color intensity at a point to obtain the PDF (Shenoy and Toor, 1988).

The PDF can also be obtained from the conversion of the acid-based reaction itself, as attempted by Wallace (1981). Shortly before that, Kappel (1979) proposed the use of decolorization reactions to obtain mixing data and presented the working equations which will be used in this work to generate PDF's and variances from previous acid-base conversion data. The equations will be derived in a simpler manner with a notation which facilitates use of the equations and gives a visual interpretation to reactive-mixing curves. In addition, Kappel's starting point, which derives from Danckwerts (1957), will be reinterpreted to eliminate certain ambiguities.

Theory

The viewpoint of Danckwerts is as follows (Danckwerts, 1957; Shenoy and Toor, 1988): mix two dilute reactants at the original concentrations, C_{AO} and C_{BO}, and consider an element of fluid in the resulting mixture which is small enough to be homogeneous. Let f be the fraction of the volume of the element which came from the original A stream, and $1\text{-}f$, the fraction from the original B stream. Then, if the reaction is $A + n\,B \rightleftharpoons$ products, by stoichiometry,

$$n(f\,C_{AO} - C_A) = (1 - f)\,C_{BO} - C_B \qquad (1)$$

This, of course, assumes either that the mixing is isolated or that the net loss of A and B from the element to the surrounding fluid balances out in some fashion.

The ambiguity in the above attractive derivation is removed when Eq. 1 is derived from the convective diffusion equations, which show that the equation is valid if the effective diffusivities of the two dilute reactants in the solvent are equal, and f is identified as the dimensionless concentration of reactant A when *no reaction takes place* (Toor, 1962; Li and Toor, 1986) (the derivation is outlined in the Appendix). Thus, if the reactant diffusivities can be treated as equal, the time- and position-dependent

function f in Eq. 1 can be considered to be the instantaneous dimensionless concentration of the passive tracer, A, and it is the PDF of this quantity which will be obtained from the reactive-mixing data. A perfect instantaneous probe measurement with A as the inert tracer would then measure this same PDF, which is independent of the reaction and depends only upon the mixing. Although an equivalent derivation for unequal diffusivities is not available, reactive mixing experiments suggest that Eq. 1 can be taken to be valid over a range of nonequal diffusivities (Mao and Toor, 1971).

In the nondimensional form used earlier (Li and Toor, 1986; Shenoy and Toor, 1988), Eq. 1 becomes

$$x_A - \beta x_B = (1 + \beta) f - \beta \tag{2}$$

If the reaction between A and B is fast enough compared to the mixing, the reaction is effectively at equilibrium everywhere. If the reactants are a strong acid and strong base, then the equilibrium relationship is

$$x_A x_B = K_W / C_{AO} C_{BO} \tag{3}$$

and Eqs. 2 and 3 together relate x_A and x_B explicitly to f so that, given the PDF, usually assumed Gaussian (Hawthorne et al., 1949; Toor, 1962), one can relate the *conversion* of these instantaneous reactions to the mean and variance of the passive tracer, the nonreacting A.

For the practical dilute concentrations used, 10^{-2}–10^{-3} normal, the righthand side of Eq. 3 is close enough to zero so the reaction can be treated as irreversible, as was done in earlier reactive-mixing work which had as its goal the prediction of the time-average reaction rate from the mixing and chemistry (Vassilatos and Toor, 1965; Mao and Toor, 1971).

In this work the process is inverted—rather than use the mixing (PDF) to determine conversion, use the conversion to determine the PDF. For this purpose it is advantageous to define new nondimensional quantities as follows:

$$W_A = n C_A / (n C_{AO} + C_{BO}) = x_A / (1 + \beta) = (1 - u) x_A \tag{4}$$

$$W_B = C_B / (n C_{AO} + C_{BO}) = \frac{\beta}{1 + \beta} x_B = u x_B \tag{5}$$

$$u = C_{BO} / (n C_{AO} + C_{BO}) = \beta / 1 + \beta \tag{6}$$

Equation 2 now becomes

$$W_A - W_B = f - u \tag{7}$$

Because $W_A W_B \simeq 0$ from Eq. 3, and W_A and W_B are nonnegative, Eq. 7 gives

$$W_B = 0 \quad \text{and} \quad W_A = f - u \quad \text{for } f > u \tag{8a}$$

and

$$W_A = 0 \quad \text{and} \quad W_B = u - f \quad \text{for } f < u \tag{8b}$$

Since the reaction occurs on surfaces distributed throughout the fluid where both W_A and W_B are zero, the physical picture corresponds to a segregated system with reaction surfaces (defined by $f = u$) separating regions of fluid which contain species A from regions containing species B. (Actually, if the reaction is instantaneous, it can be shown from Eq. 15 in Li and Toor (1986) that the reaction occurs in thin sheets of thickness in f space of order $\sqrt{K_W}(1 - u)/nC_{AO}$).

Since W_A and W_B are functions of f only (once the experimental conditions like u are fixed), the time-averaged concentrations of the reactants at a fixed point are given by

$$\overline{W}_A(u) = \int_0^1 W_A(f, u) \Phi(f)\, df \tag{9a}$$

$$\overline{W}_B(u) = \int_0^1 W_B(f, u) \Phi(f)\, df \tag{9b}$$

Substituting from Eq. 8,

$$\overline{W}_A(u) = \int_u^1 (f - u) \Phi(f)\, df \tag{10a}$$

and

$$\overline{W}_B(u) = \int_0^u (u - f) \Phi(f)\, df \tag{10b}$$

The second integration can be avoided by using the time-averaged form of Eq. 7,

$$\overline{W}_A - \overline{W}_B = \bar{f} - u \tag{11}$$

Equations 10a and b are linear integral equations which must be solved for $\Phi(f)$. Specifically, Eq. 10b is Volterra's equation of the first kind (Margenau and Murphy, 1956).

If the shape of the PDF is known, then integration of Eq. 10a or 10b with this distribution would give $\overline{W}_A$ or $\overline{W}_B$ (or, equivalently, the conversion). Toor (1962) obtained such a result by a method first used by Hawthorne et al. (1949), which involves assuming that the concentration fluctuations are distributed around the mean in a Gaussian manner. Integration of Eq. 10a *assuming* a Gaussian PDF, gives this result in a more convenient form than earlier:

$$\overline{W}_A = (\sigma/\sqrt{2}) \operatorname{ierfc} [(u - \bar{f})/\sqrt{2}\,\sigma] \tag{12}$$

so if the PDF is *known* to be Gaussian, one measurement of $\overline{W}_A$ is sufficient to give the variance. However, measurement of PDF's by the passive scalar technique shows that they can be quite non-Gaussian (Tutu and Chevray, 1973; Larue and Libby, 1974; Konrad, 1976; Birch et al., 1979; Grandmaison et al., 1982; Pitts and Kashiwagi, 1984) and they are obviously non-Gaussian close to a reactor inlet, so there may be practical as well as theoretical reasons for their study.

Solution of Integral Equations, Determination of PDF

The starting point is Eq. 10. Differentiating Eqs. 10a and 10b with respect to u at a fixed point gives

$$\int_u^1 \Phi(f)\, df = -\frac{d\overline{W}_A}{du} \tag{13a}$$

$$\int_0^u \Phi(f)\, df = \frac{d\overline{W}_B}{du} \tag{13b}$$

Equations 13a and 13b may be used to obtain the cumulative probability distribution functions on a "more than (the lower limit)" and a "less than (the upper limit)" basis, respectively.

A second differentiation gives the PDF:

$$\Phi(u) = \frac{d^2\overline{W}_A}{du^2} = \frac{d^2\overline{W}_B}{du^2} \tag{14}$$

This equation was obtained by Kappel (1979) in a somewhat different form, although his intermediate steps did not allow him to readily extract the cumulative functions which will be useful subsequently.

Determination of the Variance

The intensity of segregation was defined by Danckwerts (1952) as the variance of f normalized by its initial value, but the simpler variance is used in this discussion. By definition,

$$\sigma^2 = \overline{(f-\bar{f})^2} = \bar{f}^2 - \overline{f^2} = \int_0^1 f^2\Phi(f)\,df - \bar{f}^2 \tag{15}$$

Equations 14 and 15 give

$$\overline{f^2} \equiv \int_0^1 f^2\Phi(f)\,df = \int_0^1 u^2\Phi(u)\,du = \int_0^1 u^2\frac{d^2\overline{W}_A}{du^2}\,du \tag{16}$$

Integrating by parts and using Eq. 13a,

$$\overline{f^2} = -u^2\left[\int_u^1 \Phi(f)\,df\right]\Big|_0^1 - 2\int_0^1 u\frac{d\overline{W}_A}{du}\,du \tag{17}$$

The first term of Eq. 17 disappears at both limits; the remaining term, when integrated by parts, gives

$$\overline{f^2} = -2\left[u\,\overline{W}_A\Big|_0^1 - \int_0^1 \overline{W}_A\,du\right] \tag{18}$$

As $\overline{W}_A = 0$ at $u = 1$, the first term vanishes. Then, substituting into Eq. 15, the final equation for the calculation of the variance is

$$\sigma^2 = 2\int_0^1 \overline{W}_A\,du - \bar{f}^2 \tag{19}$$

Equation 19 was derived by Kappel (1979) by a different route and not explicitly in terms of $\overline{W}_A$. It will be seen in the next section that the above form of the variance equation gives the reactive mixing plot (in the form of $\overline{W}_A$ vs. u) a nice visual interpretation.

The equation for computing the variance from the $\overline{W}_B$ data is obtained by combining Eqs. 11 and 19 to give

$$\sigma^2 = 2\int_0^1 \overline{W}_B\,du - (1-\bar{f})^2 \tag{20}$$

Equations 19 and 20 allow calculation of the variance without predetermining the PDF, an advantage in that it avoids more error-prone numerical differentiation (Ketter and Prawel, 1969).

Since the computation of the PDF, as well as the variance, requires the same reactive mixing plots, we examine the salient features of these plots next.

Reactive Mixing Plots

The reactive mixing measurements may be plotted as $\overline{W}_A$ vs. u or $\overline{W}_B$ vs. u curves (Figures 1 and 2). For the sake of concreteness, only the $\overline{W}_A$ vs. u curve will be discussed, since analogous arguments apply to the other. The solid line in Figure 1 shows a typical $\overline{W}_A$ vs. u curve for a position where the mean is $\bar{f}$. The limiting cases of "complete segregation" and "complete mixing" are shown as lines labelled CS and CM, respectively.

Intercepts. At $u = 0$ there is no B, so A behaves like a passive tracer, and it follows from Eq. 4 that

$$\overline{W}_A|_{u=0} = (\bar{c}_A/c_{AO})|_{\text{noB}} = \bar{f} \tag{21}$$

so an estimate of $\bar{f}$ may be obtained (without performing a nonreacting tracer experiment) by extrapolating the reactive mixing data to obtain the $\overline{W}_A$-intercept at $u = 0$. It is obvious from Eq. 4 that the other intercept is given by

$$\overline{W}_A|_{u=1} = 0 \tag{22}$$

Limiting behavior. For the limiting case of "complete segregation" (i.e., zero diffusion, no molecular mixing at all), species A can be treated as an inert tracer, so that $\bar{c}_A/c_{AO} = \bar{x}_A = \bar{f}$, as before. Thus, from Eq. 4, this case will result in the straight line whose equation is

$$\overline{W}_A^{CS} = (\bar{c}_A/c_{AO})(1-u) = \bar{f}(1-u) \tag{23}$$

Before analyzing the other extreme of "complete mixing," it is necessary to know the criteria for species A and B to be limiting reactants. From Eqs. 4, 5, and 11,

- If $u = \bar{f}$, then $\bar{c}_B = n\bar{c}_A \rightarrow A$ and B are in stoichiometric proportion.
- If $u > \bar{f}$, then $\bar{c}_B > n\bar{c}_A \rightarrow A$ is the limiting reactant.
- If $u < \bar{f}$, then $\bar{c}_B < n\bar{c}_A \rightarrow B$ is the limiting reactant.

In the limit of "complete mixing," the limiting reactant will

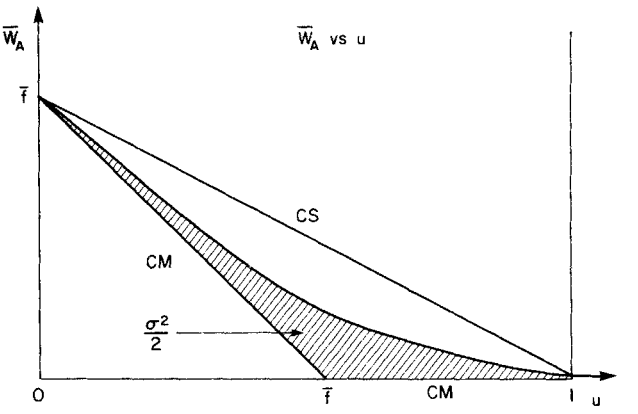

Figure 1. Typical reactive mixing plot in terms of species A.

σ^2 = twice the shaded area

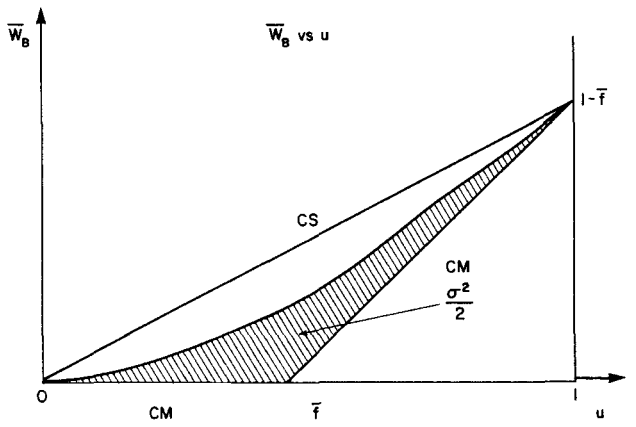

Figure 2. Typical reactive mixing plot in terms of species *B*.

σ^2 = twice the shaded area

be entirely consumed. Equation 11 then suggests that

$$\overline{W}_A^{CM} = \begin{cases} \bar{f} - u & \text{for } u \le \bar{f} \\ 0 & \text{for } u \ge \bar{f} \end{cases} \tag{24}$$

Clearly, the actual $\overline{W}_A$ vs. u and $\overline{W}_B$ vs. u curves lie between the above two limits of "complete segregation" and "complete mixing." The curves may be closer to the CM or the CS lines, depending on how well mixed the reactor position under consideration is. As a matter of fact, from Eqs. 19 and 20 the variance is just twice the area between the actual $\overline{W}_A$ or $\overline{W}_B$ curve and the "completely mixed limit" straight lines. This geometrical significance of the variance in terms of the shaded areas (Figures 1 and 2) adds an attractive visual quality to these plots.

The Limiting Case of Complete Segregation

It may appear puzzling, at first glance, to obtain $\Phi(u) = 0$ by using Eq. 14 and differentiating Eq. 23 twice. However, Eqs. 13a and 13b can be put to use in this case. Differentiating Eq. 23 and its B analog and inserting the results into Eqs. 13a and 13b, shows that for any value of u, the cumulative distribution functions on a "more than" and "less than" basis, is equal to $\bar{f}$ and $(1 - \bar{f})$, respectively. These conclusions suggest that the PDF for the "completely segregated" case consists of two Dirac delta functions of area $(1 - \bar{f})$ and $\bar{f}$, located at $f = 0$ and $f = 1$, respectively, In mathematical form,

$$\Phi^{CS}(f) = (1 - \bar{f})\delta(f - 0) + \bar{f}\delta(f - 1) \tag{25}$$

The variance computation, which involves only integration, can be done three different ways: by substituting the $\overline{W}_A^{CS}$ and $\overline{W}_B^{CS}$ expressions into Eqs. 19 and 20, respectively, or by inserting Eq. 25 into the variance definition provided by Eq. 15. Thus, for "complete segregation,"

$$(\sigma^2)^{CS} = \bar{f}(1 - \bar{f}) \tag{26}$$

The Limiting Case of Complete Mixing

For the "completely mixed" case, the $\overline{W}_A^{CM}$ vs. u and the $\overline{W}_B^{CM}$ vs. u curves have a "cusp" at $u = \bar{f}$. Equation 24, along with Eqs. 13a and 14, indicate that the cumulative distribution function jumps from 1 to 0 at $f = \bar{f}$; so, the PDF is a Dirac delta function of unit area located at $u = \bar{f}$, which may be represented by:

$$\Phi^{CM}(f) = \delta(f - \bar{f}) \tag{27}$$

As before, the variance can be obtained by integration, following one of three possible approaches. Clearly, for this case, $\sigma^2 = 0$, as the root-mean-square concentration fluctuations go to zero as the limit of "complete mixing" is approached.

The above discussion on limiting cases suggests that any Dirac delta functions in the PDF, which typically pose difficulties, can be handled with the procedure suggested in this section.

We now concentrate on the application of the PDF equation (Eq. 14) and the variance equation (Eq. 19) to data which were obtained in early reactive mixing studies in one-dimensional reactors (Vassilatos, 1964; Mao, 1969).

Results and Discussion: One-dimensional Reactor

Vassilatos (1964) developed a multijet mixing head that had a concentration field effectively uniform on a coarse scale (i.e., independent of radial distance) and nonhomogeneous over a long enough axial distance. The multiinjection head with 97 parallel stainless-steel tubes in a square array was expected to yield a uniform flow field with a relatively flat velocity profile, although McKelvey et al. (1975) showed that this was not the case near the inlet, due to back flow near the wall. Mao (1969) studied a multijet head similar to that of Vassilatos, but used 188 tubes in a close-packed arrangement. The two feeds were introduced through alternate tubes of the mixing head into a tubular reactor and the conversion was determined by measuring the temperature rise along the centerline of the reactor (Vassilatos and Toor, 1965; Mao and Toor, 1971). Since the reactants were strong acids and strong bases, the reactions were effectively instantaneous. The conversion at fixed points was measured as a function of β (Vassilatos, 1964; Vassilatos and Toor, 1965; Mao, 1969; Mao and Toor, 1971), so $\overline{W}_A(u)$ is known at various axial position for various values of u.

In a one-dimensional reactor, $\bar{f}$, is a constant and is equal to the volumetric flowrate fraction of the stream containing species A, or in this case, the acid. The volumetric flowrates of the feeds were equal in Vassilatos' and Mao's experiments, so $\bar{f} = 0.5$. The variance may be computed from Eq. 12 for a one-dimensional reactor, if a *Gaussian* PDF is assumed and if the reactants are fed in stoichiometric proportions (i.e., $u = \bar{f}$). Then, Eq. 12 simplifies to

$$\sigma^2 = 2\pi(\overline{W}_A^{SR})^2 \tag{28}$$

where superscript SR denotes a stoichiometric feed. Comparing the values of the variance obtained from Eqs. 28 and 19 will provide useful information on the validity of the Gaussian assumption for the PDF.

Vassilatos (1964) measured the conversion at eight axial positions, using seven different values of the feed concentration ratio, β. Because the system is symmetric with respect to the reactants, as was Mao's, each measurement for $\beta \neq 1$ yields two data points on the $\overline{W}_A(u)$ plot (for each point at u there is a corresponding point at $1 - u$). Thus, Vassilatos' data gives thirteen points at eight axial positions. Figure 3 shows the data (that has

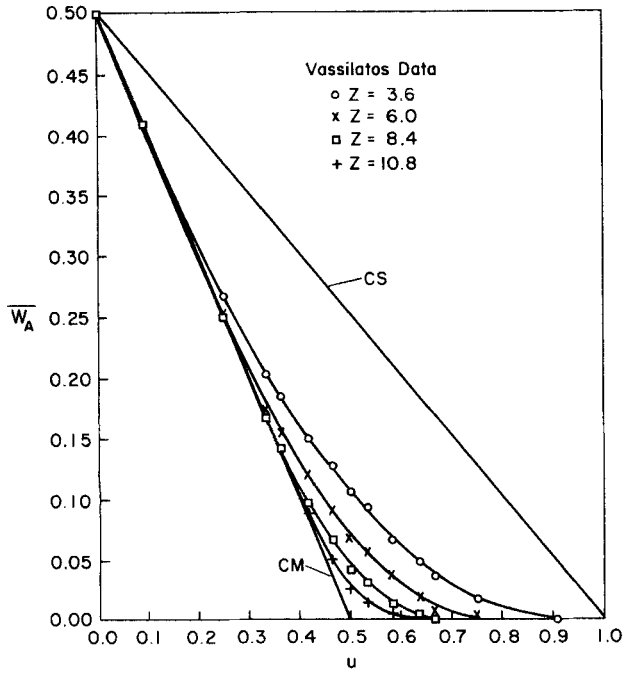

Figure 3. Reactive mixing plot for Vassilatos' data.

very little scatter) along with the fitted curves for the first four of these eight stations. The IMSL routine ICSSCV performs a cubic spline smoothing to generate curves which provide excellent fits to the data. As expected, the curves lie between the limiting cases of "complete segregation" and "complete mixing" which exist at the reactor inlet and far downstream, respectively, and as one moves downstream, the variance (the shaded area in Figure 1) is seen to be tending towards zero.

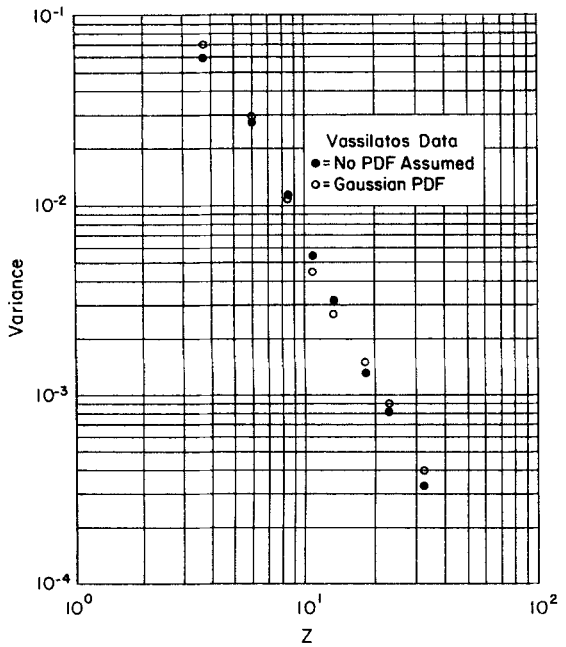

Figure 4. Variance from Vassilatos' data with and without Gaussian assumption.

Figure 4 shows that the values for the variance, computed from Eq. 19 by the IMSL routine DCSQDU (Cubic Spline Quadrature), are fairly close to those obtained from Eq. 28, which assumes a Gaussian PDF. Obviously, the variance decreases with axial distance downstream, since the concentration fluctuations decay to zero as the system becomes more and more mixed.

The PDF profiles obtained from Eq. 14 using the IMSL routine DCSEVU (Cubic Spline First/Second Derivative Evaluator) are shown for the eight different downstream distances in Figure 5, which also gives the measured fractional conversion at each position. For stations closer to the inlet, the PDF is a relatively flat and broad curve, whereas for positions far downstream, the PDF is a sharply peaked curve. A check can be made on the PDF by computing the area under the PDF curve. The areas obtained by numerical integration are given in Figure 5 and are within 3% of unity in most cases.

Sufficiently close to the inlet of the reactor, there will be completely unmixed acid ($f = 1$) and base ($f = 0$), so two Dirac delta functions of areas a_1 and a_0 must be present, $a_1\delta(f-1)$ and $a_0\delta(f-0)$, which evolve far downstream into a single delta function, $\delta(f-\bar{f})$. The closeness of the areas to one suggests that by the first station, 3.6 jet diameters downstream, the delta functions have mostly disappeared so there is little totally unmixed (virgin) fluid left.

McKelvey (1968) and McKelvey et al. (1975) measured instantaneous tracer concentrations in a replica of Vassilatos' reactor and his PDFs are compared in Figure 6 with the two from Figure 5 which are at positions common to McKelvey. Although the absolute values of McKelvey's variances are not available, the *normalized* values are indistinguishable from those obtained from Eq. 12 with Vassilatos' data (McKelvey et al., 1975). According to the Kolmogorov-Smirnov test (Owen, 1962), at the 95% confidence level, none of the PDFs can be distinguished from the Gaussian curve or from each other.

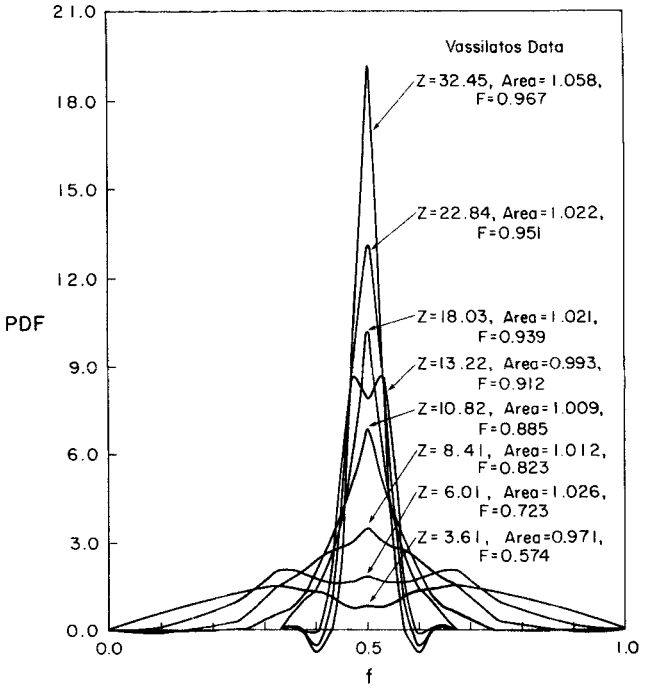

Figure 5. PDF's from Vassilatos' data.

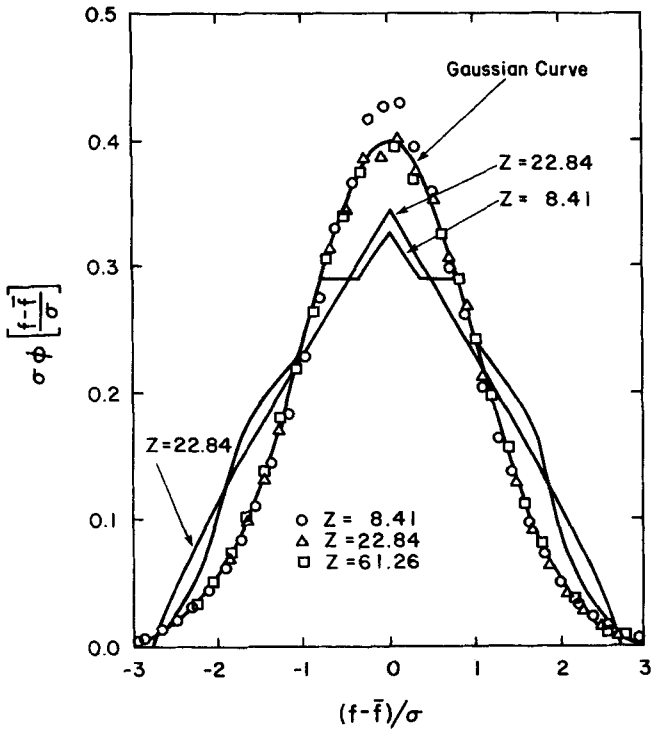

Figure 6. PDF's from Vassilatos' data vs. direct measurements by McKelvey.
Data points and Gaussian curve from McKelvey (1968)

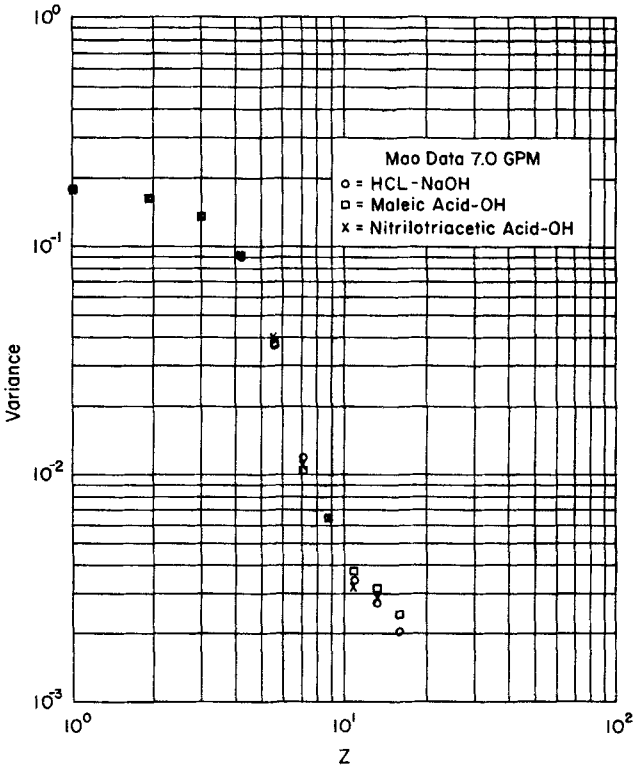

Figure 8. Variances from Mao's data for three different acid-base reactions.

Even though Mao's (1969) experimental measurements result in only five data points on the $\overline{W}_A$ vs. u plot (obtained from his data at three values of β), ten usable axial positions were investigated by him, including some very close to the inlet. For clarity, only the data and the cubic spline curve fits for the first

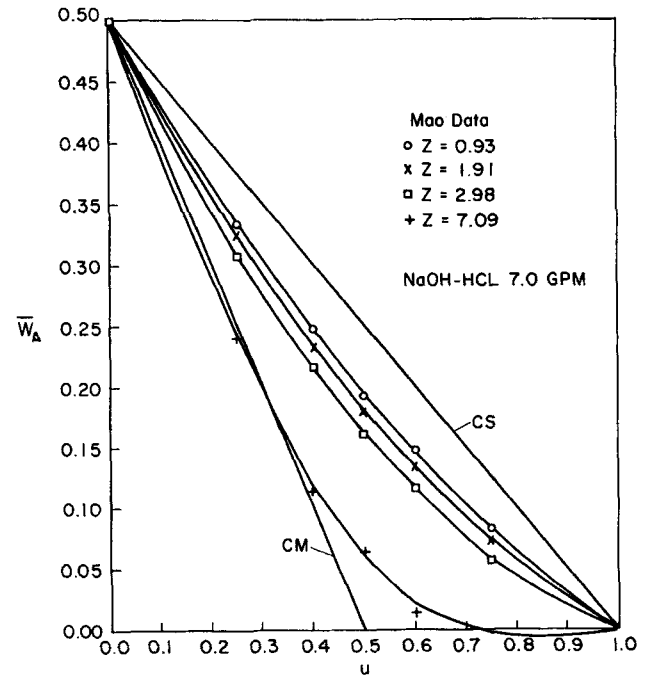

Figure 7. Reactive mixing plot from Mao's data.

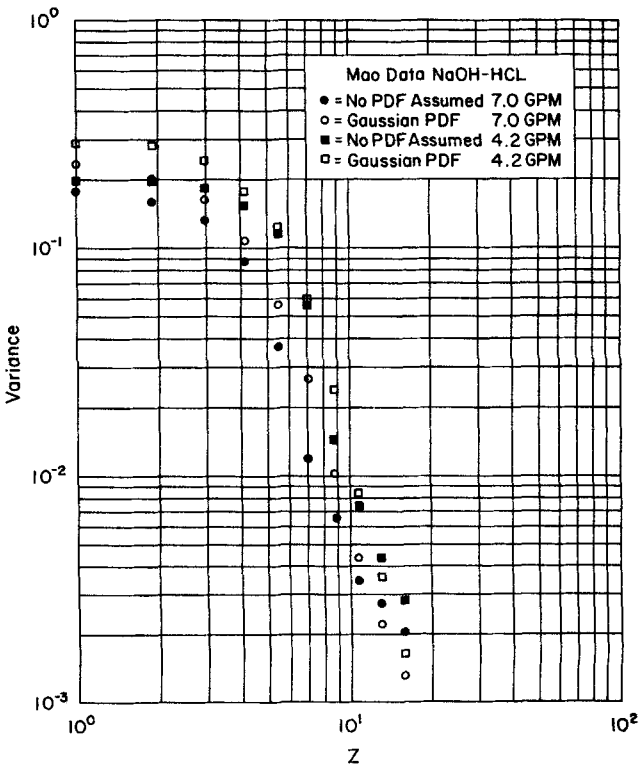

Figure 9. Variances from Mao's data with and without Gaussian assumption for two different flowrates.

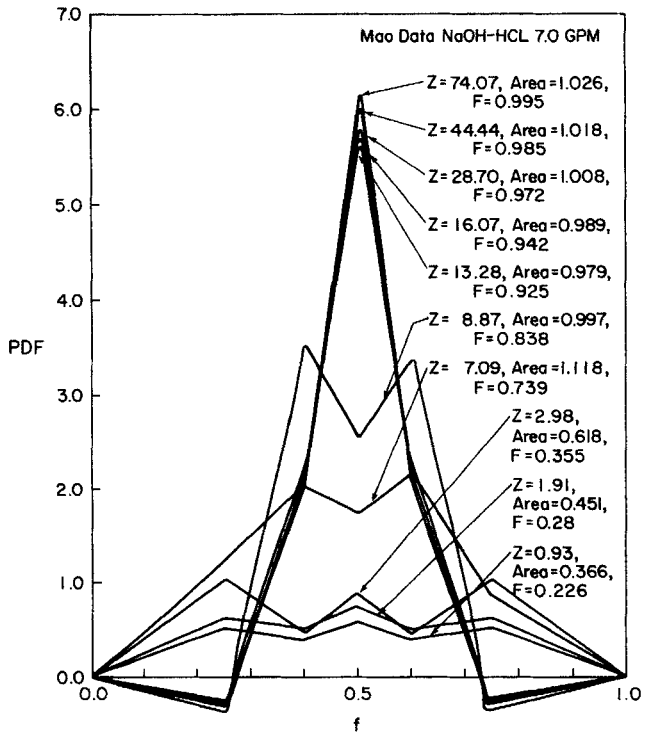

Figure 10. PDF's from Mao's data.

four of the ten locations, are shown in Figure 7. Since numerical integration is relatively stable, no difficulty was encountered in computing the variance, despite the limited data. Figure 8 shows the values of the variance for three different very rapid reactions studied by Mao. There does not appear to be any significant difference among them, which is evidence in favor of the equal diffusivity assumption. Figure 9, which compares variance values from Eqs. 19 and 28 for two different flowrates, suggests that the PDF in Mao's case is not as Gaussian as that in Vassilatos' case, a conclusion also reached by Mao (1969). The PDF profiles in Figure 10 (which also gives the measured fractional conversions), calculated as before, do not appear as promising as those of Vassilatos, due primarily to the decrease in the number of data points available to carry out the numerical differentiation. The limited amount of available Mao's data and the possible inaccuracies in them lead to regions of negative probability in some of the profiles, a problem also encountered by Wallace (1981). However, the area under the PDF in Figure 10 for the first three stations is far from unity, which is possible evidence of the existence of delta functions—unmixed virgin fluid in which $f = 0$ or 1. But this is also implied in Figure 7 because it follows from Eq. 13 that if $(d\overline{W}_A)/(du)$ does *not* go to minus one when u goes to zero, there is probably a Dirac delta function in the PDF at $f = 0$, and if $(d\overline{W}_A)/(du)$ does *not* go to zero when u goes to one, there is probably a delta function at $f = 1$. Thus, the missing area under the PDF in Figure 10 should be the area under these two delta functions which are given by Eq. 13a as,

$$\text{area of Dirac delta function (at } f = 0) = a_0 = 1 + \left.\frac{d\overline{W}_A}{du}\right|_{u=0} \tag{29}$$

$$\text{area of Dirac delta function (at } f = 1) = a_1 = -\left.\frac{d\overline{W}_A}{du}\right|_{u=1} \tag{30}$$

These areas were obtained from Eqs. 29 and 30 by differentiating the earlier spline fits in Figure 7, and the results are in Table 1. The areas at $f = 0$ and $f = 1$ are equal, as expected, and the total area $(a_0 + a_1)$ from Eqs. 29 and 30 equals the area missing from the PDF's in Figure 10, which can be taken as a check on the consistency of the numerical methods.

In spite of the consistency of the above results, it is unlikely that PDF's which have Dirac delta functions at $f = 0$ and $f = 1$ would go to zero at these borders, as they appear to do at the first three stations in Figure 10. Rather, continuity considerations suggest that these PDF's should curve upwards as the borders are approached and that the zeros at the borders are a consequence of the sparse data near the borders. If this is the case, then the values of the delta functions in Table 1 include not only the virgin fluid at $f = 0$ and 1 but also the near-virgin fluid which cannot be seen with available data.

Although the methods of this paper are general enough to be applicable to two-and three-dimensional systems, suitable data for testing them in such systems do not appear to be available.

Acknowledgment

This work was supported by National Science Foundation Grant No. CBT-8505378.

Appendix: Derivation of Eq. 1

The derivation follows Toor (1962) and Li and Toor (1986). Two dilute reactants in a common incompressible solvent at initial concentrations, C_{AO} and C_{BO}, react as they are steadily mixed. If the reactant diffusivities are equal and the reaction is $A + nB \rightleftharpoons$ products, then the convective diffusion equations together with the stoichiometry give

$$L(C_A) = L(C_B/n) = r_A \tag{1A}$$

Table 1. Dirac Delta Functions in Mao's PDF Profiles

Axial Distance Downstream z/d	a_0, Area of "Dirac Delta Function," $f = 0$	a_1 1 Area of "Dirac Delta Function," $f = 1$	Sum of Two "Dirac Delta Functions	"Missing" Area Under PDF, Figure 10
0.93	0.3174	0.3173	0.635	0.634
1.91	0.2746	0.2746	0.549	0.549
2.98	0.1913	0.1913	0.383	0.382

where

$$L = \frac{\partial}{\partial t} + \underline{V} \cdot \nabla - D\nabla^2 \tag{2A}$$

By subtraction,

$$L(nC_A - C_B) = L(C_t) = 0 \tag{3A}$$

So the quantity, C_t, is conserved by the reaction as is a nonreacting tracer which is used to characterize the mixing. Component A becomes this tracer when $C_{BO} = 0$, so it satisfies the same conservation law as C_t. Therefore, when A and B are dilute enough to have no effect on the fluid properties,

$$L(C_A^0) = L(C_t) = 0 \tag{4A}$$

Because the above equations are linear and homogeneous, nondimensional forms of C_A^0 and C_t will satisfy the equations, and these nondimensional quantities can be chosen to satisfy the same boundary conditions as follows:

Let subscripts 1 and 2 refer to the initial A and B streams, respectively, so $C_{A1} = C_{AO}$, $C_{B1} = 0$, $C_{A2} = 0$, and $C_{B2} = C_{BO}$. Then define

$$f = \frac{C_A^0 - C_{A2}}{C_{A1} - C_{A2}} = \frac{C_A^0}{C_{A0}} \tag{5A}$$

$$g = \frac{C_t - C_{t2}}{C_{t1} - C_{t2}} = \frac{nC_A - C_B + C_{BO}}{nC_{AO} + C_{BO}} \tag{6A}$$

f and g obviously satisfy the same boundary conditions—both are one where A enters, zero where B enters, and both have their normal derivatives, zero, on all solid surfaces. And since both also satisfy Eq. 4A,

$$L(f) = L(g) \tag{7A}$$

Since f and g satisfy the same differential equation and the same boundary conditions, they must be equal, so

$$g = f \tag{8A}$$

or, with Eq. 6A,

$$\frac{nC_A - C_B + C_{BO}}{nC_{AO} + C_{BO}} = f \tag{9A}$$

which is Eq. 1 in a slightly different form.

Manuscript received Oct. 5, 1988, and revision received July 10, 1989.

Notation

a_0, a_1 = areas of Dirac delta functions in PDF at $f = 0$ and $f = 1$, respectively
A,B = reactants
C = concentration, gmol/L
C_A^0 = concentration of nonreacting tracer, gmol/L
$C_t = nC_A - C_B$
D = diffusivity, cm^2/s
f = dimensionless concentration of nonreacting tracer, C_A^0/C_{AO}, in absence of reaction or volume fraction of A stream
F = fractional conversion
K_W = ion product of water, 10^{-14} (mol/L)^2
L = defined by Eq. 2A
n = stoichiometric coefficient
t = time, s
u = defined by Eq. 6
V = velocity vector, cm/s
W_A, W_B = dimensionless reactant concentrations, defined by Eqs. 4 and 5
x_A, x_B = C_A/C_{AO}, C_B/C_{BO}
Z = dimensionless axial distance downstream in jet diameters

Greek letters

$\beta = C_{BO}/n\,C_{AO}$
Φ = probability density function of the nonreacting tracer
σ^2 = variance
δ = Dirac delta function

Subscripts

A, B = reacting species
O = initial value in feed
1, 2 = A and B streams, respectively

Superscripts

— = time-averaged (or space-averaged)
CS = complete segregation
CM = complete mixing
SR = stoichiometric feed

Literature Cited

Birch, A. D., D. R. Brown, M. G. Dodson, and J. R. Thomas, Jr., "Studies of Flammability in Turbulent Flows Using Laser Raman Spectroscopy," *J. Fluid Mech.*, **88**, 431 (1979).

Brodkey, R. S., "Mixing in Turbulent Fields," *Turbulence in Mixing Operations*, ed., R. S. Brodkey, Academic Press, New York (1975).

Danckwerts, P. V., "The Definition and Measurement of Some Characteristics of Mixtures," *Appl. Sci., Res., Sect. A*, **3**, 279 (1952).

———, "Measurement of Molecular Homogeneity in a Mixture," *Chem. Eng. Sci.*, **7**, 116 (1957).

Grandmaison, E. W., D. E. Rathgeber, and H. A. Becker, "Some Characteristics of Concentration Fluctuations in Free Turbulent Jets," *Can. J. Chem. Eng.*, **60**, 212 (1982).

Hawthorne, W. R., D. S. Weddel, and H. C. Hottel, *Third Symposium Combustion and Flame and Explosion Phenomena*, p. 266, Williams and Wilkins, Baltimore, MD (1949).

IMSL Library, version 9.0 edition, International Mathematical and Statistical Libraries, Inc., Houston (1982).

Kappel, M., "Development and Application of a Method for Measuring the Mixture Quality of Miscible Liquids: I. State of Research and Theoretical Principles," *Int. Chem. Eng.*, **19**, 196 (1979).

Ketter, R. L., and S. P. Prawel, *Modern Methods of Engineering Computation*, McGraw-Hill, New York (1969).

Konrad, J. H., "An Experimental Investigation of Mixing in Two-Dimensional Turbulent Shear Flows with Applications to Diffusion-Limited Chemical Reactions," PhD Thesis, Caltech and Project SQUID Tech. Rep. CIT-8-PU (1976).

Koochesfahani, M. M., and P. E. Dimotakis, "Mixing and Chemical Reactions in a Turbulent Liquid Mixing Layer," *J. Fluid Mech.*, **170**, 83 (1986).

Larue, J. C., and P. A. Libby, "Temperature Fluctuations in the Plane Turbulent Wake," *Phys. Fluids*, **17**, 1956 (1974).

Li, K. T., and H. L. Toor, "Chemical Indicators as Mixing Probes. A Possible Way to Measure Micromixing Simply," *I&EC Fund.*, **25**, 719 (1986).

Mao, K. W., "Chemical Reactions with Turbulent Mixing," PhD Diss., Carnegie Mellon University (1969).

Mao, K. W., and H. L. Toor, "Second-Order Chemical Reactions with Turbulent Mixing," *I&EC Fund.*, **10**, 192 (1971).

Margenau, H., and G. M. Murphy, *The Mathematics of Physics and Chemistry*, D. Van Nostrand Co., New York (1956).

McKelvey, K. N., "Turbulent Mixing with Chemical Reaction," PhD Diss., Ohio State University (1968).
McKelvey, K. N., M. N. Yieh, S. Zakanycz, and R. S. Brodkey, "Turbulent Motion, Mixing and Kinetics in a Chemical Reactor Configuration," *AIChE J.*, **21**, 1165 (Nov., 1975).
Owen, D. B., "Handbook of Statistical Tables," Ch. 12, Addison Wessley, Reading, MA (1962).
Pitts, W. M., and T. Kashiwagi, "The Application of Laser-Induced Rayleigh Light Scattering to the Study of Turbulent Mixing," *J. Fluid Mech.*, **171**, 27 (1984).
Shenoy, U. V., and H. L. Toor, "Micromixing Measurements with Chemical Indicators," *Proc. Eur. Conf. on Mixing*, Pavia, Italy (1988).
Toor, H. L., "Mass Transfer in Dilute Turbulent and Nonturbulent Systems with Rapid Irreversible Reactions and Equal Diffusivities," *AIChE J.*, **8**, 70 (Jan., 1962).
———, "The Non-Premixed Reaction: A + B → Products," *Turbulence in Mixing Operations* Ch. III, ed., R. S. Brodkey, Academic Press, New York (1975).
Tutu, N. K., and R. Chevray, "Temperature and Velocity Measurements in a Heated Jet," *Bulletin Am. Phys. Soc. II*, **18**, 11 (1973).
Vassilatos, G., "A Study of Very Rapid and Rapid Second Order Isothermal Irreversible Liquid Phase Reactions between Two Initially Unmixed Reactants in a Turbulent Field," PhD Diss., Carnegie Mellon University (1964).
Vassilatos, G., and H. L. Toor, "Second-Order Chemical Reactions in a Nonhomogeneous Turbulent Fluid," *AIChE J.*, **11**, 666 (July, 1965).
Wallace, A. K., "Experimental Investigation on the Effects of Chemical Heat Release in the Reacting Turbulent Plane Shear Flow," Doctoral Diss., University of Adelaide, Australia, AFOSR-TR-84-0650 (1981).

Manuscript received Oct. 5, 1988, and revision received July 10, 1989.